Origin of the spin polarization of magnetic scanning tunneling microscopy tips

Paolo Ferriani,* Cesar Lazo, and Stefan Heinze
Institut für Theoretische Physik und Astrophysik, Christian-Albrechts-Universität zu Kiel, D-24098 Kiel, Germany
(Received 10 June 2010; published 10 August 2010)

Using first-principles calculations, we demonstrate that the vacuum spin polarization of commonly used Fe-coated scanning tunneling microscopy (STM) tips is positive at the Fermi energy—opposite to that of Fe surfaces—and is often lower than expected from magnetic thin films. We consider single Fe atoms and pyramids of five Fe atoms on Fe (001) and (110) surfaces as models of STM tips. While the spin polarization of the local density of states (LDOS) at the apex atom of all considered tips is negative close to the Fermi energy and dominated by minority *d* electrons, the spin polarization of the vacuum LDOS, crucial for the tunneling current, is positive and controlled by majority states of *sp* character. These states derive from the atomic 4*s* and 4*p* orbitals and provide a large spillout of charge density into the vacuum. If we replace the Fe apex atom by a Cr, Mn, or Co atom, the vacuum spin polarization remains positive at the Fermi energy, and it is much enhanced for Cr or Mn in the favorable antiferromagnetic spin alignment with respect to the Fe tip body. At energies above the Fermi level, the spin polarization can change sign due to the contribution from antibonding minority *d* states. Single Mn and Fe atoms on a nonmagnetic tip provided, for example, by a Cu(001) surface display a similar vacuum LDOS with a small positive spin polarization in good agreement with recent experimental findings. For Cr-coated tips, we observe that the spin polarization can display a change in sign very close to the Fermi energy which can complicate the interpretation of the measured asymmetry in spin-polarized tunneling spectroscopy.

DOI: 10.1103/PhysRevB.82.054411 PACS number(s): 68.37.Ef, 71.15.Mb, 75.70.Ak

I. INTRODUCTION

The spin-polarized scanning tunneling microscope (SP-STM) has become one of the key tools in nanomagnetism.[1–3] Combining atomic-scale resolution with spin sensitivity, it allows to study the intriguing local magnetic properties of nanostructures on surfaces from ultrathin films[3–7] down to single atoms[8,9] or molecules.[10] Using the atom manipulation capability of STM opens the route to investigate the magnetic properties of artificial nanostructures designed atom-by-atom[9,11] and by contacting single atoms or molecules on surfaces with the tip their conductance can be measured.[12] Very recently, inelastic tunneling spectroscopy with a SP-STM has been applied to even control the spin state of a single atom using the spin torque exerted by a spin-polarized current.[13] Crucial to the success of all these experiments is a tip with high spin sensitivity. In most experiments, this has been achieved by coating a nonmagnetic STM tip made from W or Ir with a magnetic material such as Fe or Cr.[3] In addition, due to tip-sample interaction during scanning or intentional tip preparation,[13] single magnetic atoms or small clusters can be picked up from the sample.

Although today SP-STM is a well-established experimental technique, there has been a long debate on the origin of the spin-polarized electrons from such tips, based on two main arguments. (i) Intuitively, we would expect the *d* electrons, which are responsible for the magnetization in 3*d*-transition metals, to dominate the spin polarization (SP) at the apex atom of the tip, while *s* and *p* electrons should display only a very small spin polarization. This scenario has been proposed by Alvarado based on measurements of the tunneling current between a Ni tip and a GaAs(110) sample.[14,15] The dominance of minority *d* states leading to a negative spin polarization in scanning tunneling spectroscopy (STS) measurements also holds for many ferromagnetic ultrathin films and surfaces of 3*d*-transition metals, e.g., Fe/W(110),[3,16] CrFe surface alloys,[17] the Fe(001) surface,[18,19] and Co films on Cu(111),[20,21] on Cu(001),[19] and on Pt(111).[22]

On the other hand (ii), above the apex atom in the vacuum region the local density of states (LDOS), the key quantity for the tunneling current, may be dominated by the more delocalized *s* and *p* electrons. However, due to their small exchange splitting and small DOS at the atom, we would not expect a significant contribution to the spin polarization of the tunneling current. Nevertheless, for states far above the Fermi energy, evidence has been given that also *s* and *p* states can give rise to a considerable spin polarization of the tunneling current for single atoms on surfaces,[23] which can be regarded as a simple model of the tip apex structure. It has been reported that 3*d*-transition-metal atoms on fcc-(111) surfaces possessing a surface state can display a splitoff state of *s*-orbital character with a large vacuum LDOS and positive spin polarization.[24–26] Moreover, high spin-polarization enhancement has been found upon H atom adsorption at the apex of a Cr-coated tip.[27] Recently, the spin-dependent orbital character of states from a single magnetic Co atom has been imaged using SP-STM (Ref. 9) demonstrating the competition of majority *sp* states and minority *d* states. Based on these findings, a tunneling current dominated by *sp* states might not be incompatible with high tip spin polarization.

Here, we use first-principles calculations based on density-functional theory to shed light onto this key issue of SP-STM and discuss ways to improve the choice of magnetic tips to enhance the magnetic resolution. Especially if the sample possesses only a small spin polarization, the quality of the tip decides about the success of the experiment. Our results also apply to single magnetic atoms on magnetic surfaces which have recently moved into the spotlight of re-

search on nanostructures at surfaces. We present first-principles calculations of Fe- and Cr-based STM tips considering different tip structures, surface orientations, and adsorbed 3*d*-transition-metal atoms. For comparison, we have also performed calculations for single magnetic adatoms on nonmagnetic surfaces. We have evaluated the LDOS and its spin polarization in the vacuum which are the essential quantities in the tunneling current within the Bardeen approach to STM.[28] We focus on the case of small bias voltages, which is relevant for magnetic resolution at the atomic scale and crucial for inelastic tunneling spectroscopy which has recently received much attention[11,29–34] and has also been combined with spin sensitivity.[13]

Surprisingly, we find for Fe-based tips with a single protruding apex atom that it is not the minority *d* electrons which give rise to high spin polarization of the vacuum LDOS but rather the majority electrons with *sp* character resulting in a significant positive spin polarization in the vicinity of the Fermi energy. This unexpected effect can be understood on the basis of *sd* hybridization at the apex atom. A comparison with the clean iron (100) and (110) surfaces is in accordance with this interpretation and emphasizes the role of the symmetry and the local environment at the tip apex. Replacing the Fe apex atom by other 3*d*-transition metals such as Cr, Mn, Co, and Ni leads to a similar spin polarization. Above the Fermi level, we observe a change in sign of the spin polarization which can complicate the interpretation of the measured asymmetry in spin-polarized tunneling spectra. This effect is particularly striking for Cr(001)-based tips which display the change in sign at the Fermi energy.

This paper is organized as follows. In Sec. II we give the computational details of the method used to calculate the electronic structure of STM tips. In Sec. III, we first discuss our analysis of the spin polarization of the electronic states starting from the Fe(001) and Fe(110) surfaces as reference cases which we compare with tips of single Fe atoms and small Fe clusters on these surfaces. We then turn to single Cr, Mn, Co, and Ni atoms on Fe(001). In addition, we compare our results with those for single Mn and Fe atoms on nonmagnetic Cu(001) surface, as it has recently been demonstrated that individual Mn atoms on Cu tips show spin sensitivity at low temperature upon stabilizing the magnetic moment in an external magnetic field.[13] In the last section, we study a simple model for Cr-based tips. A summary and conclusions finalize our paper.

II. METHOD

The electronic and magnetic structure of magnetic STM tips has been studied from first-principles based on density-functional theory calculations in the generalized gradient approximation (GGA).[35] We apply the full-potential linearized augmented plane-wave method as implemented in the FLEUR code.[36] We used the film geometry that provides a highly accurate description of the potential and wave functions in the vacuum region up to 10 Å above the surface.[37] The tips have been modeled by a five layer film with a single atom or a pyramid composed of a four-atom base and an apex atom in the $c(4\times4)$ two-dimensional (2D) unit cell. Due to the large employed 2D unit cell we can exclude interaction between periodic replica of the tips. The theoretical GGA lattice constant of Fe ($a=5.38$ a.u.) has been used. Structural relaxations have been performed for every system based on force minimization (forces below 10^{-3} hartree/a.u.). We used 125 basis functions per atom and applied three (four) special k points in the irreducible part of the 2D Brillouin zone for the (100) [(110)]-based tips. The muffin-tin radius of the apex cluster atoms was 2.15 a.u. We have checked our results with respect to slab thickness, exchange-correlation potential, energy, and special k points cutoff and found no qualitative influence on the results discussed here.

In order to relate the electronic structure of the STM tip and the tunneling current we apply the Bardeen approach to STM.[28] The central quantity in this theory is the matrix element between states ψ_μ of the sample and χ_ν of the tip evaluated at the separation surface between tip and sample. The influence of the electronic structure of the tip on the tunneling current can thus be analyzed by calculating its spin-dependent LDOS and spin polarization approximately 3 to 7 Å above the apex atom. On this basis we can compare different magnetic STM tips and relate the spin polarization of the LDOS to the electronic states at the apex atom of the tip. We define the SP of the vacuum LDOS according to

$$P(z,\epsilon)=\frac{n^{\uparrow}(z,\epsilon)-n^{\downarrow}(z,\epsilon)}{n^{\uparrow}(z,\epsilon)+n^{\downarrow}(z,\epsilon)}, \tag{1}$$

where $n^{\sigma}(z,\epsilon)$ is the LDOS of the spin channel $\sigma\in\{\uparrow,\downarrow\}$ at a distance z from the apex atom and at an energy ϵ with respect to the Fermi level. In the spirit of the surface integral for the Bardeen tunneling current, we integrate the LDOS in the vacuum over the 2D unit cell.

III. RESULTS

A. Fe(001) surface

Prior to investigating the spin polarization of the STM tip, it is instructive to recall the properties of a simple well-known system that has been extensively studied both theoretically and experimentally, namely, the Fe(001) surface. The LDOS of the surface atoms of Fe(001), Fig. 1(a), shows the typical behavior of a ferromagnet with large spin splitting of the majority and minority *d* bands. The majority band is essentially full, with the Fermi level, E_F, located at its tail while the minority *d* band is nearly half occupied, i.e., E_F is at the center of the band. As a result, the LDOS around the Fermi energy is dominated by minority electrons, in particular, by surface states and resonances, and the spin polarization is negative.

The different contributions of *s*, *p*, and *d* electrons to the LDOS can be separated by plotting its orbital decomposition, which is shown in Fig. 1(b) around the Fermi energy. The 4*s* band shows a strong dispersion and provides an almost constant contribution in the whole energy range. On the contrary, the more localized *d* states generate a narrow band with large peaks overwhelming the contribution of the *s* electrons. This is evident for the minority band in the considered energy range. In the majority channel, however, the *d* states lie

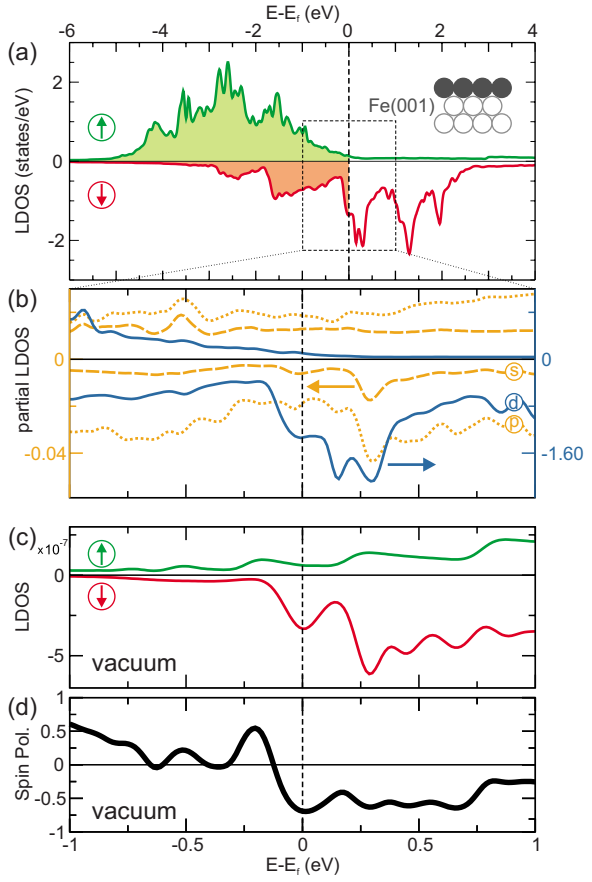

FIG. 1. (Color online) LDOS of the Fe(001) surface. (a) LDOS in the muffin-tin sphere of a surface atom and (b) its orbital decomposition in the vicinity of the Fermi energy. Note that the scale for *sp* and *d* states differs by a factor of 40. (c) LDOS in the vacuum region calculated at 5.7 Å from the surface atoms and (d) its spin polarization. The Fe(001) surface has been modeled with a 19-layer slab.

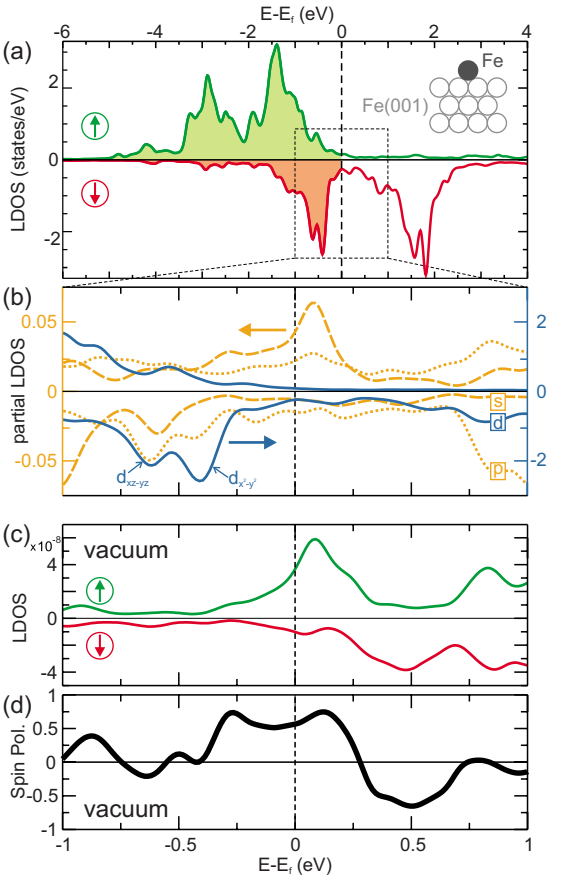

FIG. 2. (Color online) LDOS of the Fe adatom on the Fe(001) surface. (a) LDOS in the muffin-tin sphere of the Fe adatom. (b) Orbital decomposition of the LDOS in the vicinity of the Fermi energy. Note that the scale for *sp* and *d* states differs by a factor of 40. (c) LDOS in the vacuum region evaluated at 5.9 Å from the adatom and (d) its spin polarization.

at lower energies due to the exchange splitting, and the LDOS from the *d* electrons is much reduced around E_F, while *s* and *p* states are of similar magnitude.

The spin-resolved LDOS in the vacuum at about 5.7 Å above the surface, Fig. 1(c), displays quite a different shape, owing to the state-dependent decay in the vacuum barrier. Nevertheless, the qualitative picture of the spin polarization discussed for the surface layer holds. The minority channel clearly dominates, with the largest contribution coming from the peak at about +0.3 eV. This is the well-known d_{z^2} surface state, which represents the characteristic signature of the Fe(001) surface in STS.[18] From a comparison with the peak energies in Fig. 1(b) we infer that the minority states in the vacuum stem from *d* electrons. The Fe(001) surface clearly illustrates the crucial importance of considering the LDOS in the vacuum for the interpretation of STM measurements.

Due to the lack of majority *d* states near E_F, the vacuum LDOS shows the onset of the *sp* band.[38] The vacuum spin polarization is given by the imbalance of the spin-up and spin-down LDOS as seen in Fig. 1(d). The spin polarization is strongly negative and nearly constant up to 0.75 eV above E_F. Below the Fermi energy, a change in sign is observed due to the onset of the majority *d* band [cf. Fig. 1(a)], however, it remains rather small in the considered energy range. This finding supports the idea that the large number of *d* states at the surface atoms results in a LDOS in the vacuum of *d* character albeit the localized character of *d* states. Recently, the negative spin polarization of Fe(001) around E_F has also been confirmed by inelastic spin-polarized scanning tunneling spectroscopy[19,39] and a value of −61% has been given in good agreement with the value of −69%, which we extract from Fig. 1(d).[40]

B. Fe atom on the Fe(001) surface

A simple model of a magnetic STM tip is given by a single Fe atom adsorbed in the hollow site of an Fe(001) surface. This idealized geometry already captures a key ingredient of any STM tip, namely, the local environment of the apex atom, protruding out of the tip body. In the following, we will show that considering more complex tip structures such as small pyramids does not affect our general conclusions from this section.

An analysis of the LDOS similar to the one performed for the Fe(001) surface in the previous section is displayed in

Fig. 2. The lower coordination number of the Fe adatom results in narrower 3*d* bands, which split into bonding and antibonding states, and the suppression of the d_{z^2}-surface state. In the majority-spin channel, we observe an *sp* resonance slightly above E_F originating from the 4*s* state of the free Fe atom [see Fig. 2(b)]. Another *sp* resonance is located at about 0.8 eV above E_F. However, the LDOS in the vicinity of E_F is still dominated by minority *d* electrons due to their much larger absolute value [note the different scale for *sp* and *d* states in Fig. 2(b)]. In this respect, the single Fe atom is similar to the Fe(001) surface and the spin polarization of the LDOS at the adatom is negative.

In the vacuum region, the situation is quite different. The *sp* resonances in the majority channel contribute significantly to the vacuum LDOS as a result of their larger delocalization, as seen in Fig. 2(c), and are of similar magnitude as the minority *d* states. Therefore, the spin polarization is reversed close to the Fermi energy and amounts to 56%. In the unoccupied states, the sign of the spin polarization is first reversed owing to the antibonding minority *d* states and approaches zero at the second *sp* resonance. The *sp* resonance in the majority channel is similar to the one reported by N. Lang for a Mo adatom on a metallic surface described within the jellium model.[41] However, due to the spin-split density of states of Fe and the *sd* hybridization, it is found only in the majority-spin channel at E_F and therefore plays an important role for the tip spin polarization.

A real-space plot of the LDOS in the vicinity of the Fermi level, Fig. 3, allows a direct visualization of the involved electronic states. The different orbital character of majority and minority states is revealed by a cross section of the LDOS in a plane parallel to the surface shown in Fig. 3(b). The former exhibits a rotationally symmetric state with a maximum at the adatom position, characteristic of the *s*, p_z, and d_{z^2} states, while the latter has the typical fourfold symmetry of a $d_{x^2-y^2}$ state with a node at the center. This picture is confirmed by the cross sections of the LDOS parallel to the tip axis displayed in Fig. 3(c). It is evident that the different orbital character of majority and minority states plays a crucial role in the sign of the spin polarization. The majority *sp* state propagates along the *z* direction while the minority $d_{x^2-y^2}$ state spreads parallel to the surface. A different orbital symmetry of states in the two spin channels shown here has recently also been observed experimentally by spin-polarized STM for single Co adatoms adsorbed on a Mn monolayer on the W(110) surface.[9] A similar shape of the charge density as in Fig. 3 was reported based on first-principles calculations for 3*d*-transition-metal adatoms on W(001).[42,43]

From Fig. 3(c) we also deduce a different bonding character of the states in the two spin channels. The majority states exhibit charge depletion in the region between the tip apex atom and the neighboring atoms, with a large amount of electron-density spilling out into the vacuum. This is consistent with the location of the Fermi level at the high-energy tail of the *d* band, corresponding to antibonding states [cf. Fig. 2(a)]. On the contrary, the position of the Fermi level below the pseudogap of the minority band suggests a bonding character, which is confirmed by the charge accumulation in the region between the apex atom and the surface atoms

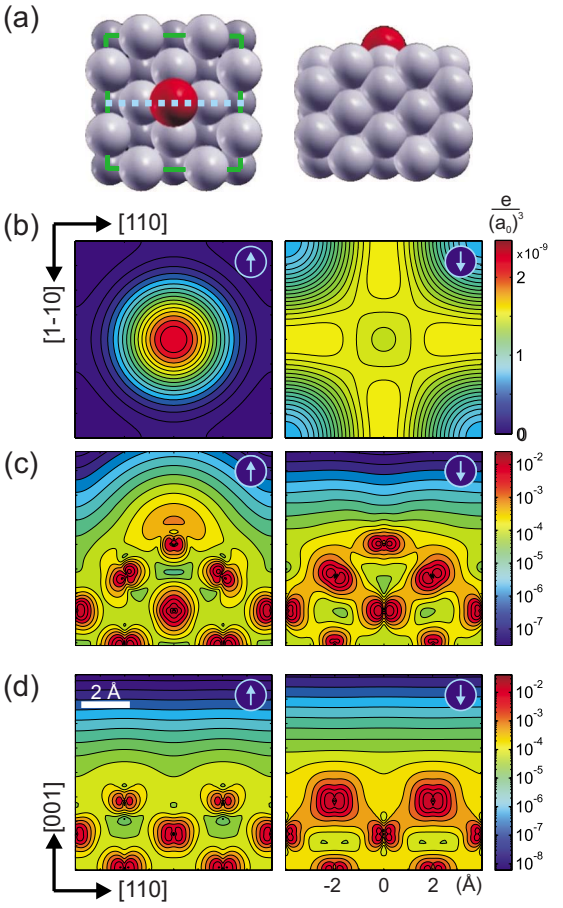

FIG. 3. (Color online) Spin-dependent LDOS for states in the energy range between E_F and E_F+100 meV for an Fe adatom on Fe(001) and the Fe(001) surface. (a) 2D unit cell of the Fe adatom on Fe(001) in a top (left) and side view (right). (b) Cross section of the vacuum LDOS in the majority (left) and the minority channel (right) in a plane parallel to the surface at a distance of 5.9 Å from the adatom. (c) Cross section of the LDOS in a plane perpendicular to the surface along the dotted line given in (a). (d) Perpendicular cross section of the LDOS for the Fe(001) surface. a_0 is the Bohr radius.

underneath, with only little contribution to the vacuum. For comparison, the LDOS at the Fermi energy is displayed for the Fe(001) surface in Fig. 3(d). In this case, majority and minority states are also of *sp* and *d* characters, respectively, but decay similarly into the vacuum. Due to the larger minority LDOS at the surface atoms the vacuum spin polarization is negative.

Because the rotationally symmetric spin-up state for the Fe atom on the Fe(001) surface dominates in the vacuum, the spin-averaged as well as the spin-polarized LDOS exhibits a circular shape, as shown in Figs. 4(a) and 4(b). From the cross-sectional plot of the spin-averaged LDOS [Fig. 4(c)] we see that at the tip apex atom the $d_{x^2-y^2}$ state prevails.

Therefore, the spin-polarized LDOS possesses a spatial dependence and must show a crossover as we move from the Fe adatom into the vacuum [Fig. 4(d)]. The reversal of the spin polarization occurs at only 1 Å from the apex atom as seen from Fig. 5. In the vacuum region beyond about 3 Å from the apex atom the spin polarization remains nearly con-

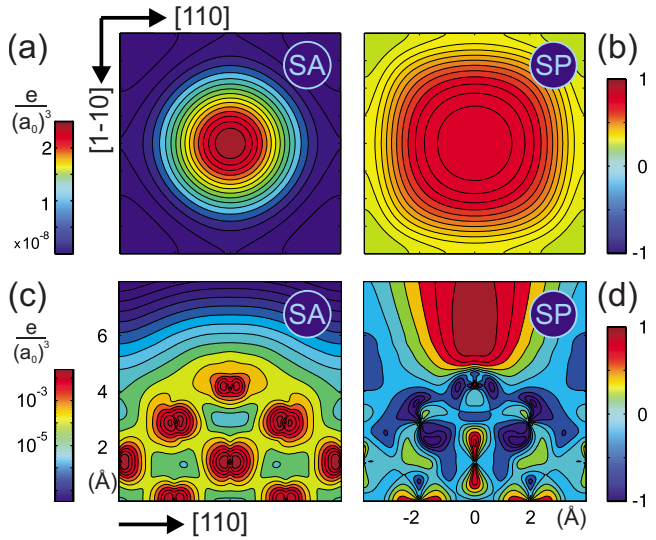

FIG. 4. (Color online) Cross section of the (a) vacuum spin-averaged LDOS $[n^{\uparrow}(\mathbf{r},\epsilon)+n^{\downarrow}(\mathbf{r},\epsilon)]/2$ and (b) of the local spin polarization $P(\mathbf{r},\epsilon)$ [cf. Eq. (1)] for an Fe adatom on Fe(001) in the energy range between E_F and E_F+100 meV evaluated in a plane parallel to the surface at a distance of 5.9 Å from the adatom. In (c) and (d) the same quantities as in (a) and (b), respectively, have been evaluated in a plane perpendicular to the surface along the [110] direction.

stant. The spin-polarized LDOS also exhibits a spatial dependence in the lateral direction, cf. inset of Fig. 5. We have analyzed this dependence quantitatively by varying the extent of the 2D integration parallel to the surface for the vacuum spin polarization at E_F as shown in Fig. 5. We observe a qualitatively similar trend for all curves. However, the absolute value of the spin polarization can change by a factor of almost 2 if we compare the two extreme cases. Although in the Bardeen model of the tunneling current the integral over tip and sample states is performed on a separation surface in the vacuum region, using the vacuum LDOS for both sides is a simplification. Nevertheless, the curves for the distance-dependent spin polarization of the vacuum LDOS are very similar to the conductance obtained in the tunneling regime based on a tight-binding calculation between two Fe(001)-based atomic-size contacts.[44] A competition between slowly decaying 4*s* orbitals in the majority and fast decaying 3*d* states in the minority channel at the Fermi energy has also been found in that study.

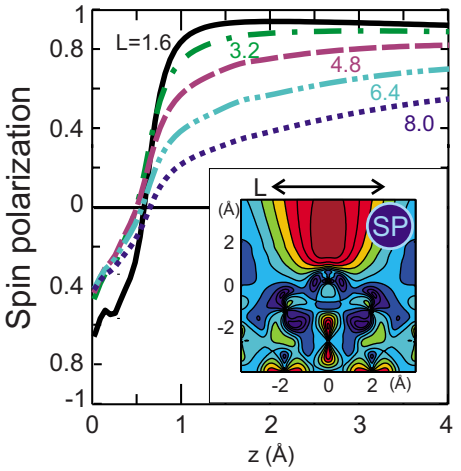

FIG. 5. (Color online) Spatial dependence of the vacuum spin polarization for a single Fe atom on Fe(001) evaluated in the energy range between E_F and E_F+100 meV as a function of the distance from the apex atom for different length L of the integration interval along the [110] direction.

In conclusion, we find a more complicated behavior of the vacuum spin polarization for the Fe adatom than for the Fe(001) surface which originates from the competition of majority *sp* states and minority *d* states. The positive spin polarization around E_F occurs due to the different orbital symmetry and bonding character of majority and minority states resulting in a faster decay of the minority states into the vacuum.

C. Fe clusters on Fe(001) and Fe(110)

In order to understand in how far the conclusions we obtained in the previous section apply more generally to Fe tips, we have extended our study to other geometrical conformations at the tip apex. These calculations also provide valuable information about how the tip properties are influenced upon structural modifications at the apex induced, e.g., by pulsing the tip or due to interaction with the sample.

In Fig. 6 we present a summary of the spin polarization of the vacuum LDOS for the different tip structures we considered. Panels (a) and (b) display the spin polarization for the Fe(001) surface and the Fe adatom on Fe(001), respectively, which were already given in Figs. 1 and 2. The reversal of the spin polarization at the Fermi energy which we discussed in the previous section is evident from these two plots. If we now consider an Fe pyramid with a four-atom base on the Fe(001) surface, Fig. 6(c), we obtain a spin polarization qualitatively similar to the case of the single Fe atom, cf. panel (b), i.e., a positive spin polarization around E_F and a strong reduction for the occupied states. Analyzing the LDOS at the Fe apex atom of the pyramid confirms that the positive spin-polarization stems from a similar *sp* state as for the single Fe atom but shifted here to about 0.3 eV above E_F.

We can demonstrate the crucial impact of the single protruding Fe atom for the positive spin polarization by removing it from the Fe pyramid as shown in Fig. 6(d). This geometry is an intermediate case between the single atom and the bare Fe(001) surface and the spin polarization is close to zero in an energy range of about 0.5 eV around E_F. The atomic-like *sp* state is absent and the spin polarization is small due to the competition of minority *d* states and majority *sp* and *d* states. The breaking of the surface symmetry induced by a single atomic protrusion induces a change in the orbital character of the majority electrons that prevail in the vacuum region. Our interpretation is substantiated by the calculation for the Fe pyramid on Fe(001) showing a similar spin-dependent orbital character of the states at E_F, namely, a rotationally symmetric *sp*-like state in the spin-up channel and a $d_{xz,yz}$ character in the spin-down channel (not shown).

For a bcc crystal such as Fe the most densely packed surface is given by the (110) orientation which is therefore

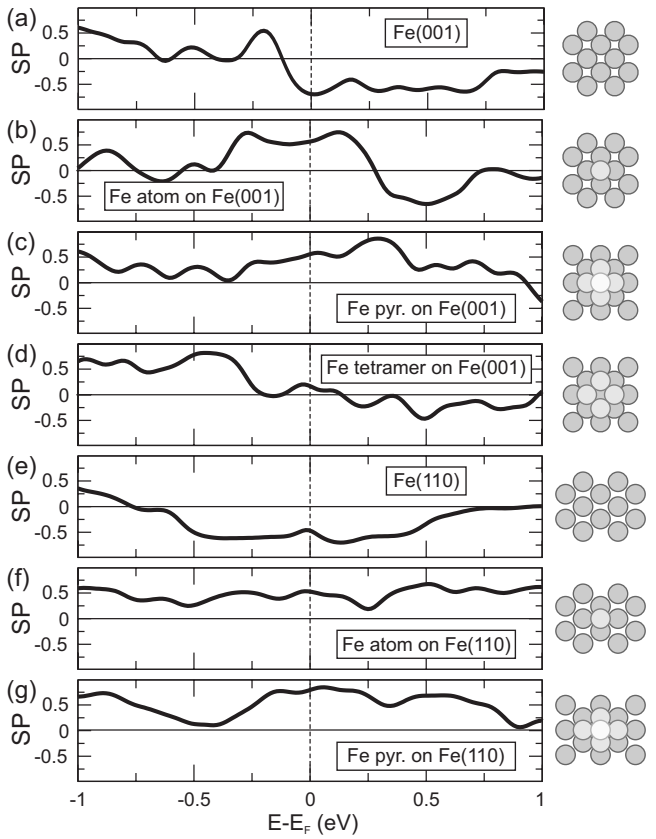

FIG. 6. Spin polarization of the vacuum LDOS at a distance of about 6 Å from the topmost atom for Fe clusters on Fe surfaces. The cluster configuration is shown by small sketches on the right side. (a) Fe(001) surface. (b) Fe adatom on Fe(001). (c) Five-atom Fe pyramid on Fe(001). (d) Four-atom Fe base on Fe(001). (e) Fe(110) surface. (f) Fe adatom on Fe(110). (g) Five-atom Fe pyramid on Fe(110).

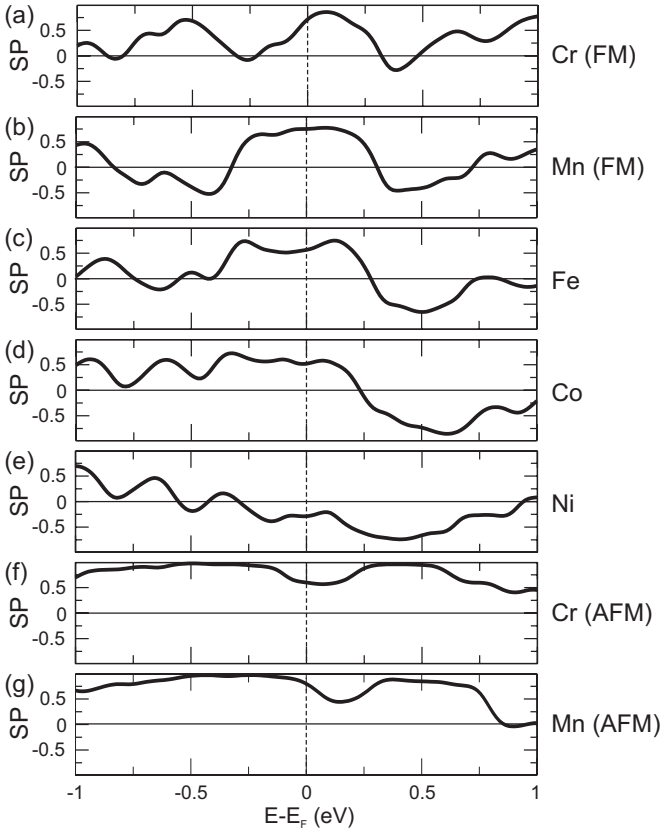

FIG. 7. Spin polarization of the vacuum LDOS for single 3*d*-transition-metal atoms on Fe(001) evaluated at a distance of about 6 Å from the adatom. (a)–(e) correspond to a ferromagnetic configuration. The results for the antiparallel alignment of the magnetic moment of the Cr and Mn adatom to the one of the Fe(001) surface are shown in (f) and (g).

also a probable local tip structure. Our results for such (110)-based tips confirm the scenario concluded from the (001) orientation: while the bare Fe(110) surface displays a negative spin polarization at the Fermi energy [Fig. 6(e)] stemming from minority *d* states, the presence of an apex atom such as a single adatom or a five-atom pyramid [Figs. 6(f) and 6(g), respectively] reverses the spin polarization to a positive value in the vicinity of E_F. Here, the *sp* resonances are broader in energy than for the (001) based tips due to a stronger hybridization on the (110) surface resulting in a wider regime of positive spin polarization. The shape of the spin polarization of the single adatom and the five-atom pyramid is also quite similar indicating the central importance of the local environment of the apex atom. Therefore, considering larger pyramids to model the tip geometry would not modify our conclusions on the character of the states and the positive spin polarization in the vacuum. Further support for this notion comes from recent tight-binding calculations for the conductance of ferromagnetic atomic-size contacts.[44] A plot of the LDOS at the Fermi energy analogous to Fig. 3 reveals the same spin dependence of the orbital character observed above, i.e., an *sp* state of antibonding character in the majority and a *d* state in the minority-spin channel.

D. 3*d*-transition-metal adatoms on Fe(001)

In SP-STM experiments the tip composition can change due to interaction with the sample, e.g., in soft tip crashes, when pulsing the tip, or in atom manipulation experiments. Thereby, material from the sample, which typically differs from the tip, can be adsorbed at the tip apex or tip material can be lost. Naturally, the question arises whether such a change in the atomic species of the foremost atom induces substantial modifications of the tip properties, e.g., of the tip spin polarization. In order to address this issue, we investigated Fe-based tips in which the tip apex atom has been substituted by another 3*d*-transition-metal atom, ranging from Cr to Ni. Based on the conclusions from the previous section, i.e., that the simple model of an adatom captures the main features of the spin polarization for a magnetic tip, we focus on single 3*d*-transition-metal atoms on Fe(001) and did not consider more complex geometries.

In Figs. 7(a)–7(e) we present the vacuum spin polarization for single Cr, Mn, Fe, Co, and Ni atoms on Fe(001), respectively. We consider first a ferromagnetic alignment of the magnetic moments of the adatom and the Fe(001) surface, which is the ground state for Fe, Co, and Ni adatoms. With the exception of Ni, all the curves show a very similar overall behavior, with a large positive polarization around

the Fermi level and a spin-polarization reversal between +0.25 and +0.35 eV with respect to E_F. The positive spin polarization around the Fermi energy stems from an *sp* resonance in all the systems. We further observe a monotonic shift of the sign reversal at positive energies as we move across the 3*d* series, which originates from the increasing 3*d*-band filling. Therefore, the picture of a competition between majority *sp* states and minority *d* states which controls the spin polarization in the vicinity of E_F holds quite generally.

Only for a Ni apex atom a small negative spin polarization at E_F is found, which is a consequence of the almost filled minority *d* band that shifts the antibonding *d* states to the Fermi energy. Note that this result is consistent with the conclusion reached from the experimental finding reported by Alvarado for Ni bulk tips.[14,15]

For Cr and Mn adatoms on Fe(001), an antiferromagnetic (AFM) coupling to the Fe(001) surface is actually the energetically preferred state. We observe a considerable modification of the vacuum spin polarization due to this magnetic ordering as displayed in Figs. 7(f) and 7(g). The spin polarization remains positive and interestingly approaches the fully spin-polarized limit and is almost constant in a wide energy range. Therefore, such tips seem very favorable from an experimental point of view.

We can understand this result from an analysis of the LDOS presented for the Mn atom on Fe(001) in Fig. 8. The LDOS of the Mn adatom in the AFM coupling can be explained based on the model of covalent magnetism,[45,46] which leads to a larger DOS of the bonding *d* states in the majority channel and a much smaller one in the minority-spin channel and vice versa for the antibonding *d* states. The antibonding majority-spin states are mostly occupied and overlap with the 3*d* bands of the Fe surface, Fig. 8(a). For the minority electrons, the Fermi energy lies in between the small DOS of bonding and huge DOS of antibonding states which do not overlap with the Fe bands. Therefore, the Mn majority 3*d* states extend above the Fermi energy. This is reflected also in the orbital decomposition of states close to the Fermi energy given in Fig. 8(b). In the majority channel, there appears a distinct p_z-d_{z^2} hybrid state below E_F and a broad DOS from $d_{xz,yz}$ orbitals in the unoccupied states. In the minority channel, we find much larger contributions from the unoccupied states, in particular, a *s*-d_{z^2} state slightly above E_F. From this observation we would expect the minority states to display a large contribution to the vacuum, however, we find that the majority-spin channel is dominant, cf. Fig. 8(c). One can identify a peak from the p_z-d_{z^2} hybrid state as well as the density of states due to the $d_{xz,yz}$-type orbitals. In contrast, the minority states display only small peaks in the vacuum LDOS for *sd*-hybrid states. The spin polarization is thus large and positive, and it is decreased only slightly at the positions of the minority LDOS peaks.

Concerning the states involved, this finding is similar to our discussion for the Fe adatom on Fe(001). In particular, the *sp* states which hybridize with *d* states at the upper edge of the 3*d* band provide a large contribution to the vacuum LDOS while the states at the lower edge extend only little into the vacuum. We can relate this to the bonding and antibonding characters of states in the lower and upper parts of the *d* band, respectively. For the Mn atom in the AFM state, the d_{z^2} character of the majority hybrid states is much more pronounced as it stems from the antibonding part of the *d* band that stretches across E_F. The d_{z^2}-orbital symmetry of these states should also affect the resolution obtained with such STM tips as pointed out by Chen.[47,48] This different orbital character could explain the unexpected enhanced resolution found in spin-polarized STM experiments performed on ultrathin Mn films on W(110) (Ref. 49) and W(001) (Ref. 50) if we assume that Mn atoms from the sample have unintentionally been adsorbed at the apex of the Fe-coated W tips. Due to the large spin polarization and the d_{z^2}-type states, magnetic tips with AFM coupling apex atoms such as Cr or Mn seem very favorable for SP-STM measurements with high spin sensitivity and high lateral resolution.

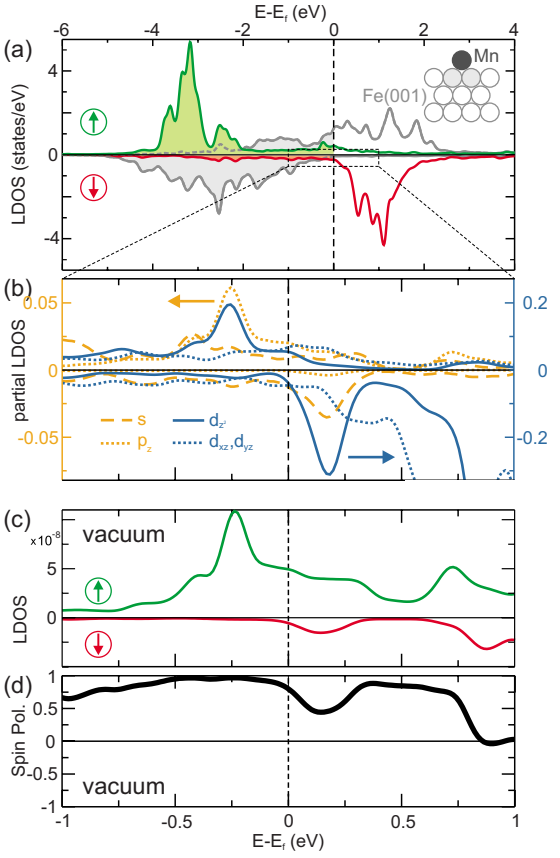

FIG. 8. (Color online) LDOS of a single Mn adatom on Fe(001) in the antiferromagnetic spin alignment. (a) LDOS at the Mn atom and the adjacent Fe surface atom (gray) for majority and minority states. (b) Orbital decomposition of the Mn LDOS in the vicinity of the Fermi energy. Only the orbitals with a large weight in the vacuum are shown. (c) Vacuum LDOS for the majority and minority states at a distance of 6.0 Å from the Mn apex atom and (d) spin polarization of the vacuum LDOS.

E. Magnetic apex atom on nonmagnetic tip body

Recently, it has been demonstrated that a single magnetic atom, e.g., Mn, adsorbed on a nonmagnetic tip made from Cu can also be used for SP-STM measurements at very low temperature ($T \approx 0.5$ K) if an external magnetic field is used

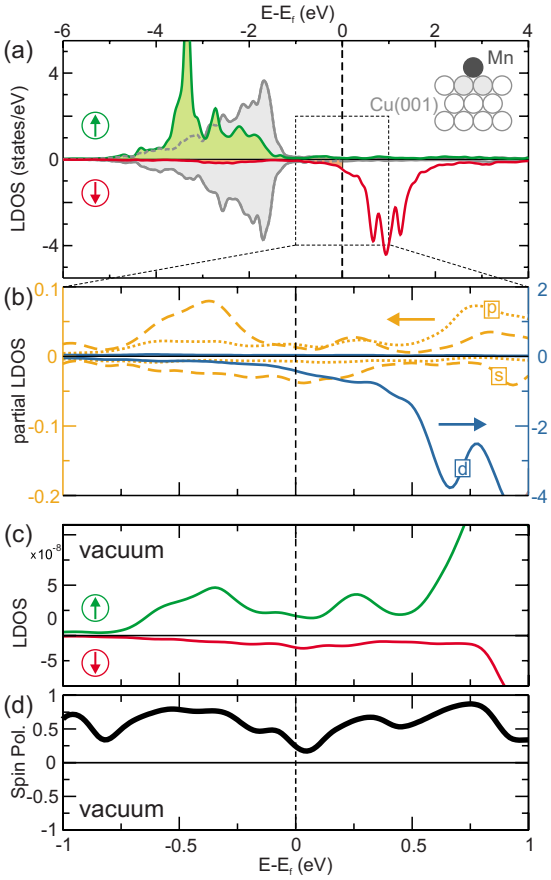

FIG. 9. (Color online) LDOS of a single Mn adatom on Cu(001). (a) LDOS at the Mn atom and at the adjacent Cu atoms (gray) for majority and minority states. (b) Orbital decomposition of the Mn LDOS in the vicinity of the Fermi energy. (c) Vacuum LDOS for the majority and minority states at a distance of 5.9 Å from the Mn apex atom and (d) spin polarization of the vacuum LDOS.

to stabilize the magnetization.[13] Therefore, we have performed a calculation for a single Mn atom on a Cu(001) surface to simulate this geometry and to compare this case to adatoms on Fe(001). As expected a large exchange splitting of majority and minority bands occurs for Mn leading to a large magnetic moment of 4.06 μ_B, cf. Fig. 9(a). Due to the hybridization with the filled 3*d* bands of the Cu substrate, the majority band of Mn lies well below the Fermi energy, and the majority LDOS at the Fermi energy is dominated by *s* and *p* states, Fig. 9(b). The minority *d* band is almost empty and only its tail extends to E_F resulting in a small negative spin polarization at the Mn atom. In the vacuum the spin-polarized LDOS in the vicinity of the Fermi energy stems from the competition between the slowly decaying *sp* states in the majority- and minority-spin channels while the minority *d* states are more localized and of bonding character. Therefore, the spin polarization is positive in the entire energy range considered in Fig. 9 but varies in size owing to the variation in the *s* states in the minority channel. For example, at the Fermi energy the spin polarization amounts to only 24%, which could explain the positive value between 20% and 30% obtained in the experiment of Loth *et al.*[13]

For single Fe atoms on Cu(001), we have found a similar trend of the spin polarization of the vacuum LDOS (not shown) with a value of about 64% at E_F. However, due to the smaller magnetic moment and earlier onset of the minority *d* band, the spin polarization changes sign at about 0.5 eV above the Fermi energy. Previously, Lounis *et al.*[24] have used first-principles calculations to study single 3*d*-transition-metal atoms on Cu(111) and found a splitoff state from the surface state of Cu(111). This effect also leads to a small positive spin polarization in the vacuum but the appearance of a surface state is restricted to an atomically flat surface and does not occur for a real STM tip. Nevertheless, we expect a similar competition of majority *sp* and minority *d* states for a Mn apex atom on a small Cu pyramid on a Cu(111) surface, similarly to Fig. 9.

F. Chromium-based tips

Finally, we will briefly discuss electronic structure effects for magnetic tips made from antiferromagnets such as chromium,[51,52] which are also popular due to the absence of magnetic stray fields that can influence the magnetic properties of the sample. Modeling such tips is much more challenging as a noncollinear magnetic structure can emerge owing to the possibility of frustration of antiferromagnetic exchange interactions in systems of reduced dimension and symmetry which inevitably occur at the apex of an STM tip. Here, we restrict ourselves to collinear magnetic configurations of chromium tips, which can be directly compared to our previous calculations for iron-based tips.

The simplest approximation of a tip is given by a single Cr atom adsorbed on the Cr(001) surface in the layerwise antiferromagnetic state. The Cr atom develops a large magnetic moment of 2.4 μ_B and couples antiferromagnetically with respect to the Cr surface atoms as seen in Fig. 10. The antiferromagnetic interaction with the Cr surface leads to a similar LDOS as for the Mn atom on Fe(001), i.e., a splitting into bonding and antibonding *d* bands in the majority and minority channels which overlap with the Cr surface bands. As expected from the model of covalent magnetism the bonding *d* band displays a very large DOS in the majority spin while it is very small for minority-spin electrons. The antibonding bands show the opposite effect. As the Fermi energy lies in between the bonding and antibonding parts of the *d* bands the vacuum LDOS above E_F is dominated by majority hybrid states of *s*, *p*, and *d* characters and the positive spin polarization reaches nearly 100%. The hybrid state of *s*, p_z, and d_{z^2} orbitals at 0.2 eV above E_F is similar to the one found below E_F for a Mn atom on Fe(001), cf. Fig. 8(b). The shift is a result of the larger band filling for Mn. The occupied minority *d* states do not display such sharp resonance features but lead to a sign reversal of the spin polarization below the Fermi energy. Due to the sharp transition from large negative to large positive values, the spin polarization is rather small at E_F. The sign change in the spin polarization at the Fermi energy may also complicate the extraction of the sample spin polarization from spin-polarized tunneling spectroscopy measurements. Note that the exact position of the sign reversal depends on the Cr

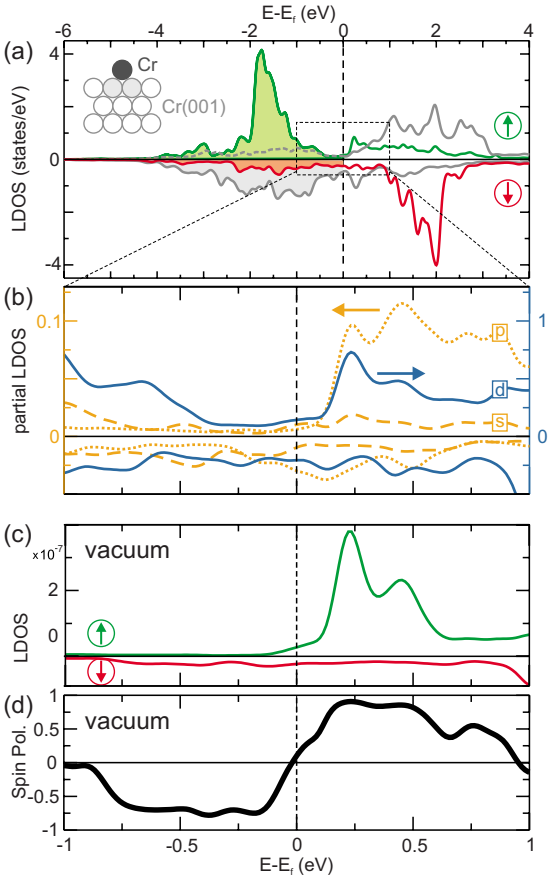

FIG. 10. (Color online) LDOS of a single Cr adatom on Cr(001) in the antiferromagnetic spin alignment. (a) LDOS at the Cr atom and the adjacent Cr surface atom (gray) for majority and minority states. (b) Orbital decomposition of the LDOS of the Cr adatom in the vicinity of the Fermi energy. (c) Vacuum LDOS for the majority and minority states at a distance of 5.9 Å from the Cr apex atom and (d) spin polarization of the vacuum LDOS.

magnetic moment, which is notoriously difficult to describe within the local-density approximation or generalized gradient approximation.[18,53]

For comparison, we have also considered a single Cr atom on the Cr(110) surface with a $c(2\times2)$ antiferromagnetic structure. The adsorbed Cr atoms then couples antiferromagnetically with respect to the nearest-neighbor Cr surface atoms. Interestingly, the calculated spin polarization of the vacuum LDOS is positive and amounts to about 47% at E_F. Its variation with energy is quite small in the range between −0.6 and 0.4 eV around the Fermi energy and is similar to that observed for a single Fe atom on Fe(110), cf. Fig. 6.

IV. SUMMARY AND CONCLUSIONS

In summary, we have performed a first-principles study of single magnetic atoms and small clusters on magnetic and nonmagnetic surfaces as a model of the structure at the apex of magnetic STM tips used for spin-polarized measurements. We have focused on iron-based tips considering two different surface orientations, i.e., Fe(001) and Fe(110), varied the local structure at the apex from single atoms to five-atom pyramids, and compared different 3*d*-transition-metal atoms at the tip apex. We showed that the local environment of the apex atom is essential for its electronic structure and observed no qualitative difference between single adatoms and the five-atom pyramids. Based on our calculations, we found for ferromagnetic tips that the spin polarization of the local density of states in the vacuum, crucial for the spin-polarized current, is positive in the vicinity of the Fermi energy and dominated by majority states of *s*- and p_z-orbital characters. These states derive from atomic-like 4*s* states and due to *sd* hybridization occur close to the Fermi energy only in the majority states. In contrast, the LDOS at the apex atom is negative, as a consequence of the partly filled minority *d* band. However, these states are more localized at the apex atom and toward the surface as a result of their bonding character and decay quickly in the vacuum. Owing to the DOS characteristic of itinerant antiferromagnetism, the states close to the Fermi energy are dominated by antibonding majority *d* states for Cr and Mn adatoms. This leads to high positive spin polarization, which often stems from d_{z^2} states that may dramatically enhance the resolution of such tips according to Chen.[47,48]

Depending on the chemical species of the apex atom and the tip geometry, the magnitude of the positive spin polarization in the vacuum varies in a large interval ranging from 20% to 80% for the ferromagnetic tips and can reach values close to the fully polarized case for antiferromagnetic tips. Above the Fermi energy, the spin polarization eventually changes sign due to the onset of the antibonding minority *d* states. Depending on the particular tip, this sign reversal occurs at energies of 0.2–0.5 eV above E_F which will influence the spin asymmetry measured in tunneling spectroscopy in the occupied states of the sample. For chromium-based tips, this reversal is even observed at the Fermi energy which would lead to a change in measured spin asymmetry for occupied and unoccupied sample states.

For the tip materials we investigated, the structural tip configuration and apex atom species do not influence the sign of the spin polarization close to E_F, which was always positive. This should facilitate manipulation experiments with magnetic tips in which the tip configuration might change frequently. However, the atom apex species can dramatically modify the value of the spin polarization allowing to improve the magnetic sensitivity and resolution. For instance, a nearly constant and very high spin polarization over a wide energy range was found for tips with an antiferromagnetic apex atom such as Cr or Mn which may allow for quantitative analysis, i.e., using inelastic tunneling spectroscopy.

ACKNOWLEDGMENTS

Financial support from the Stifterverband für die Deutsche Wissenschaft and the German Research Foundation, DFG (Project No. HE3292/7-1) is gratefully acknowledged. Part of the computations were performed at the the North-German Supercomputing Alliance (HLRN). We also thank S. Blügel and K. von Bergmann for inspiring discussions.

*Corresponding author; ferriani@physik.uni-kiel.de

[1] R. Wiesendanger, H. J. Güntherodt, G. Güntherodt, R. J. Gambino, and R. Ruf, Phys. Rev. Lett. **65**, 247 (1990).
[2] W. Wulfhekel and J. Kirschner, Appl. Phys. Lett. **75**, 1944 (1999).
[3] M. Bode, Rep. Prog. Phys. **66**, 523 (2003).
[4] S. Heinze, M. Bode, A. Kubetzka, O. Pietzsch, X. Nie, S. Blügel, and R. Wiesendanger, Science **288**, 1805 (2000).
[5] A. Yamasaki, W. Wulfhekel, R. Hertel, S. Suga, and J. Kirschner, Phys. Rev. Lett. **91**, 127201 (2003).
[6] A. Kubetzka, P. Ferriani, M. Bode, S. Heinze, G. Bihlmayer, K. von Bergmann, O. Pietzsch, S. Blügel, and R. Wiesendanger, Phys. Rev. Lett. **94**, 087204 (2005).
[7] C. L. Gao, W. Wulfhekel, and J. Kirschner, Phys. Rev. Lett. **101**, 267205 (2008).
[8] Y. Yayon, V. W. Brar, L. Senapati, S. C. Erwin, and M. F. Crommie, Phys. Rev. Lett. **99**, 067202 (2007).
[9] D. Serrate, P. Ferriani, Y. Yoshida, S.-W. Hla, M. Menzel, K. von Bergmann, S. Heinze, A. Kubetzka, and R. Wiesendanger, Nat. Nanotechnol. **5**, 350 (2010).
[10] C. Iacovita, M. V. Rastei, B. W. Heinrich, T. Brumme, J. Kortus, L. Limot, and J. P. Bucher, Phys. Rev. Lett. **101**, 116602 (2008).
[11] C. Hirjibehedin, C. Lutz, and A. Heinrich, Science **312**, 1021 (2006).
[12] N. Néel, J. Kröger, and R. Berndt, Phys. Rev. Lett. **102**, 086805 (2009).
[13] S. Loth, K. von Bergmann, M. Ternes, A. F. Otte, C. P. Lutz, and A. J. Heinrich, Nat. Phys. **6**, 340 (2010).
[14] S. F. Alvarado and P. Renaud, Phys. Rev. Lett. **68**, 1387 (1992).
[15] S. F. Alvarado, Phys. Rev. Lett. **75**, 513 (1995).
[16] M. Bode, S. Heinze, A. Kubetzka, O. Pietzsch, X. Nie, G. Bihlmayer, S. Blügel, and R. Wiesendanger, Phys. Rev. Lett. **89**, 237205 (2002).
[17] A. Davies, J. A. Stroscio, D. T. Pierce, and R. J. Celotta, Phys. Rev. Lett. **76**, 4175 (1996).
[18] J. A. Stroscio, D. T. Pierce, A. Davies, R. J. Celotta, and M. Weinert, Phys. Rev. Lett. **75**, 2960 (1995).
[19] T. Balashov, A. F. Takács, M. Däne, A. Ernst, P. Bruno, and W. Wulfhekel, Phys. Rev. B **78**, 174404 (2008).
[20] L. Diekhöner, M. A. Schneider, A. N. Baranov, V. S. Stepanyuk, P. Bruno, and K. Kern, Phys. Rev. Lett. **90**, 236801 (2003).
[21] O. Pietzsch, A. Kubetzka, M. Bode, and R. Wiesendanger, Phys. Rev. Lett. **92**, 057202 (2004).
[22] F. Meier, K. von Bergmann, P. Ferriani, J. Wiebe, M. Bode, K. Hashimoto, S. Heinze, and R. Wiesendanger, Phys. Rev. B **74**, 195411 (2006).
[23] H. J. Lee, W. Ho, and M. Persson, Phys. Rev. Lett. **92**, 186802 (2004).
[24] S. Lounis, P. Mavropoulos, P. H. Dederichs, and S. Blügel, Phys. Rev. B **73**, 195421 (2006).
[25] B. W. Heinrich, C. Iacovita, M. V. Rastei, L. Limot, J. P. Bucher, P. A. Ignatiev, V. S. Stepanyuk, and P. Bruno, Phys. Rev. B **79**, 113401 (2009).
[26] M. Wasniowska, P. A. Ignatiev, V. S. Stepanyuk, and J. Kirschner, Phys. Rev. B **79**, 165411 (2009).
[27] W. A. Hofer, K. Palotás, S. Rusponi, T. Cren, and H. Brune, Phys. Rev. Lett. **100**, 026806 (2008).
[28] J. Bardeen, Phys. Rev. Lett. **6**, 57 (1961).
[29] A. J. Heinrich, J. A. Gupta, C. P. Lutz, and D. M. Eigler, Science **306**, 466 (2004).
[30] C. Hirjibehedin, C. Y. Lin, A. F. Otte, M. Ternes, C. Lutz, B. A. Jones, and A. Heinrich, Science **317**, 1199 (2007).
[31] A. F. Otte, M. Ternes, K. von Bergmann, S. Loth, H. Brune, C. P. Lutz, C. Hirjibehedin, and A. Heinrich, Nat. Phys. **4**, 847 (2008).
[32] T. Balashov, T. Schuh, A. F. Takács, A. Ernst, S. Ostanin, J. Henk, I. Mertig, P. Bruno, T. Miyamachi, S. Suga, and W. Wulfhekel, Phys. Rev. Lett. **102**, 257203 (2009).
[33] N. Lorente and J.-P. Gauyacq, Phys. Rev. Lett. **103**, 176601 (2009).
[34] F. Delgado, J. J. Palacios, and J. Fernández-Rossier, Phys. Rev. Lett. **104**, 026601 (2010).
[35] J. P. Perdew, K. Burke, and M. Ernzerhof, Phys. Rev. Lett. **77**, 3865 (1996).
[36] http://www.flapw.de
[37] H. Krakauer, M. Posternak, and A. J. Freeman, Phys. Rev. B **19**, 1706 (1979).
[38] The wiggles are due to the finite thickness of the slab used in the calculations.
[39] N. Papanikolaou, B. Nonas, S. Heinze, R. Zeller, and P. H. Dederichs, Phys. Rev. B **62**, 11118 (2000).
[40] Note that the different vacuum LDOS obtained in Ref. 19 using the Korringa-Kohn-Rostoker method may be due to the use of the atomic sphere approximation as pointed out in Ref. 39.
[41] N. D. Lang, Phys. Rev. Lett. **58**, 45 (1987).
[42] W. A. Hofer, J. Redinger, and R. Podloucky, Phys. Rev. B **64**, 125108 (2001).
[43] W. A. Hofer and A. J. Fischer, J. Magn. Magn. Mater. **267**, 139 (2003).
[44] M. Häfner, J. K. Viljas, D. Frustaglia, F. Pauly, M. Dreher, P. Nielaba, and J. C. Cuevas, Phys. Rev. B **77**, 104409 (2008).
[45] A. R. Williams, R. Zeller, V. L. Moruzzi, C. D. Gelatt Jr., and J. Kübler, J. Appl. Phys. **52**, 2067 (1981).
[46] A. R. Williams, V. L. Moruzzi, C. D. Gelatt Jr., J. Kübler, and K. Schwarz, J. Appl. Phys. **53**, 2019 (1982).
[47] C. J. Chen, Phys. Rev. Lett. **65**, 448 (1990).
[48] C. J. Chen, Phys. Rev. B **42**, 8841 (1990).
[49] M. Bode, M. Heide, K. von Bergmann, P. Ferriani, S. Heinze, G. Bihlmayer, A. Kubetzka, O. Pietzsch, S. Blügel, and R. Wiesendanger, Nature (London) **447**, 190 (2007).
[50] P. Ferriani, K. von Bergmann, E. Y. Vedmedenko, S. Heinze, M. Bode, M. Heide, G. Bihlmayer, S. Blügel, and R. Wiesendanger, Phys. Rev. Lett. **101**, 027201 (2008).
[51] A. Kubetzka, M. Bode, O. Pietzsch, and R. Wiesendanger, Phys. Rev. Lett. **88**, 057201 (2002).
[52] A. Li Bassi, C. S. Casari, D. Cattaneo, F. Donati, S. Foglio, M. Passoni, C. E. Bottani, P. Biagioni, A. Brambilla, M. Finazzi, F. Ciccacci, and L. Duò, Appl. Phys. Lett. **91**, 173120 (2007).
[53] G. Bihlmayer, T. Asada, and S. Blügel, Phys. Rev. B **62**, R11937 (2000).